MR-Based Cardiac and Respiratory Motion-Compensation Techniques for PET-MR Imaging

Camila Munoz, MSc*, Christoph Kolbitsch, PhD, Andrew J. Reader, PhD, Paul Marsden, PhD, Tobias Schaeffter, PhD, Claudia Prieto, PhD

KEYWORDS

• Motion compensation • Respiratory motion • Cardiac motion • PET-MR imaging

KEY POINTS

- Recently developed simultaneous PET-MR scanners have broadened the possibilities for new MR-based motion-compensation techniques in PET.
- Two approaches have been proposed to use MR-measured motion fields to reconstruct a motion-corrected PET image: post-reconstruction registration and motion-compensated image reconstruction.
- MR-based motion-correction techniques for PET imaging improve the accuracy of uptake values and increase lesion detectability and contrast.
- Validation of the techniques in clinical studies with larger cohorts of patients remains to be done.

INTRODUCTION

Continuous improvement in clinical PET scanners has allowed attainment of an intrinsic spatial resolution in the range of 2 to 5 mm full-width-at-half-maximum (FWHM).[1] In practice, however, this resolution usually cannot be achieved when imaging the thoracic and abdominal regions, in part because of physiologic motion. Bulk patient motion during long PET acquisition times, as well as cardiac and respiratory motion, can have a negative effect on image quality and therefore diagnostic accuracy in a high number of patients. In addition to producing blurring, motion can produce severe image artifacts caused by mismatches between the static attenuation map and the moving emission map.[2] In oncology, motion affects the detectability of small lesions and the accuracy of quantitative analysis, impairing diagnosis and therapy monitoring.[3,4] In cardiovascular imaging, severe attenuation map mismatches caused by motion may lead to the detection of false myocardial perfusion defects, as shown by Ouyang and colleagues[5] in **Fig. 1**.

Effects of cardiac motion are usually reduced in PET imaging by gating the acquisition into frames representing different cardiac phases. Typically, an external electrocardiogram (ECG) device is used to synchronize the acquisition with the cardiac cycle. The R-wave is used as a gating reference to estimate the cardiac phase in which each coincidence was acquired, thereby allowing the data to be sorted into near motion-free cardiac frames. This sorting can be performed retrospectively in scanners with list-mode acquisition capability, or prospectively (known as on-the-fly

Disclosure: The authors have nothing to disclose.
Division of Imaging Sciences and Biomedical Engineering, Department of Biomedical Engineering, King's College London, St. Thomas' Hospital, 4th Floor, Lambeth Wing, Westminster Bridge Road, London SE1 7EH, UK
* Corresponding author.
E-mail address: camila.munoz@kcl.ac.uk

PET Clin 11 (2016) 179–191
http://dx.doi.org/10.1016/j.cpet.2015.09.004
1556-8598/16/$ – see front matter

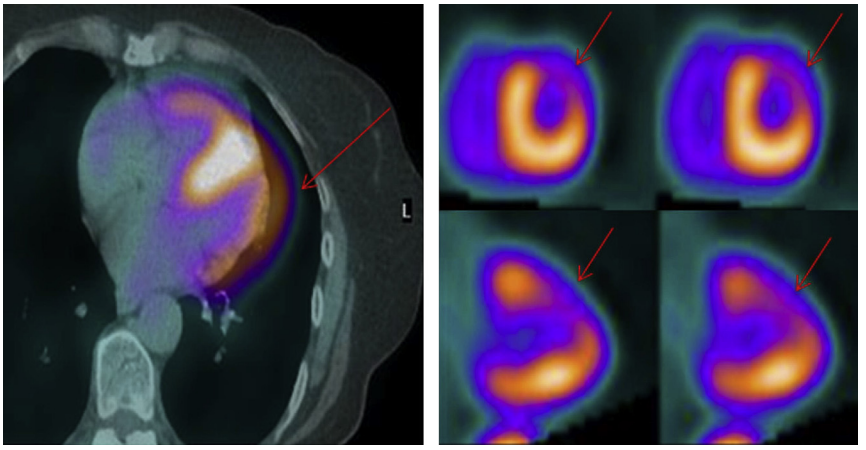

Fig. 1. Effect of motion in PET images. Arrows show an apparent myocardial perfusion defect. No stenosis was seen on subsequent catheterization or repeated imaging. (*From* Ouyang J, Li Q, El Fakhri G. Magnetic resonance-based motion correction for positron emission tomography imaging. Semin Nucl Med 2013;43:61; with permission.)

ECG-triggered acquisition). However, the signal-to-noise ratio (SNR) of each cardiac phase is highly reduced because of the low number of detected counts used in the individual reconstructions. An analogous approach can be used for respiratory motion compensation combining data acquired at similar respiratory positions from multiple breathing cycles. Usually, to measure the internal motion caused by the respiratory cycle directly is either not possible or difficult. Instead, data that can be easily measured (eg, the displacement of the skin surface) and that has a strong relationship with the motion of interest can be used as a respiratory surrogate.[6] As reviewed by Rahmim and colleagues,[1] different instrumentation solutions have been proposed to obtain a reliable surrogate signal that can be used for respiratory gating (also called binning). This includes pneumatic respiratory bellows, patient's airflow thermometers, infrared tracking systems that estimate the position of reflective markers placed in the patient's abdomen, or PET-based tracking systems where a radioactive point source is set on the patient's abdomen. Schemes that estimate a surrogate signal from PET data have also been proposed.[7] Most respiratory motion surrogates provide only qualitative information about different motion phases, which is not necessarily quantitatively linked to the motion of individual organs.

Cardiac and respiratory gating approaches have successfully been used in a wide range of static PET acquisitions,[1] where the reduced number of counts detected in each frame is compensated for by increasing acquisition time. However, this approach it is not suitable for four-dimensional (4D) dynamic PET studies. Temporal information about the radiopharmaceutical distribution is sought in 4D dynamic PET, therefore acquisition time cannot be used as a resource to improve SNR. Furthermore, external devices do not measure internal motion directly and the information obtained from them is not directly suitable for motion-correction schemes.

Motion-correction techniques are required to overcome the SNR limitations of the gating approach. Some methods that estimate motion from PET data itself have been proposed.[8,9] However, such approaches have 2 main drawbacks: they assume that changes in the activity distribution are only caused by motion and their accuracy is limited by the inherent low spatial resolution of PET images which usually depends on the uptake of the radiotracer. In combined PET-computed tomography (CT) imaging, 4D CT has been proposed to estimate the motion and correct for it in the PET reconstruction.[10–13] Motion problems can be particularly challenging in PET-CT because images with the 2 modalities can only be obtained sequentially and not simultaneously, which can lead to spatial misalignment if not adequately addressed. Moreover, even if this problem can be solved, this approach significantly increases the total radiation dose to the patient.[10]

Recently developed whole-body PET-MR scanners have broadened the possibilities for new motion-compensation techniques in PET. MR imaging provides high-resolution images and superior soft-tissue contrast compared with CT, and can be acquired truly simultaneously with PET. Well-established techniques to estimate and compensate for motion in MR imaging can be applied to PET, without increasing radiation dose or total acquisition time.[14] Moreover MR-measured motion fields can be used to

correct both the PET emission data, to reduce image blurring and increase lesion detectability, and the attenuation maps to improve quantitative accuracy of the images.

This article reviews and discusses MR-based motion-compensation techniques that have been proposed to overcome the problem of cardiac and respiratory motion in PET-MR imaging. First, an overview of MR-based motion-estimation techniques that have been used for PET-MR is given. Then different techniques for motion correction of PET images in PET-MR are described. Preliminary results of the relative impact on image quality and quantitative accuracy of motion correction compared with other correction techniques are then presented. Finally, some areas of future work are discussed.

MR-BASED MOTION ESTIMATION

Motion measurements are challenging in the thoracic and abdominal regions because of nonrigid deformations of the organs during respiratory and cardiac cycles. Different approaches have been proposed to estimate cardiac and respiratory motion, ranging from simple one-dimensional (1D) signals that can be used for data binning to complex patient-specific models that provide 4D nonrigid motion information.

Most of the proposed techniques can be divided into 2 groups: (1) precalibrated motion model techniques that acquire dynamic MR data before or during the first minutes of the PET acquisition to form a patient-specific motion model and then acquire a surrogate during the PET acquisition; and (2) simultaneous motion model techniques, where motion is estimated using MR images that are acquired throughout the whole PET acquisition process.

Cardiac Motion

In the realm of MR imaging, the most widely used techniques to estimate cardiac motion are cine-MR imaging and tagged MR imaging.[15] In cine-MR imaging, data are acquired continuously throughout several cardiac cycles and are retrospectively binned into several motion-free cardiac phases using a simultaneously acquired ECG signal. Cine-MR imaging provides information for both motion estimation and functional assessment. In terms of motion estimation for PET-MR, cine-MR imaging can be classified as a simultaneous motion model technique. Two-dimensional (2D) fast low-angle shot (FLASH) cine-MR images have been used to estimate cardiac motion in a phantom PET-MR study, using B-spline nonrigid registration of 25 cardiac phases with respect to an arbitrary reference phase.[16] Simulated three-dimensional (3D) T1-weighted images were also used by Tang and colleagues,[17] where an optical flow framework was used to estimate motion between 8 cardiac phases and the end-diastolic phase. The main drawback of the multiple 2D acquisition approach is that no information about 3D motion is available, so errors caused by misalignment between slices can be produced. Furthermore, motion is difficult to track in regions with uniform contrast such as the myocardium.

In tagged MR imaging, radiofrequency prepulses are used to generate a pattern of alternating bright and dark stripes. The most commonly used tagged MR imaging techniques are based on spatial modulation of magnetization (SPAMM), proposed by Axel and Dougherty,[18] where the deformation of a sinusoidal pattern superimposed on 2D images can be used to visualize and track motion. The pattern fades after the tagging prepulse as a result of relaxation processes, so multiple acquisitions are required in order to characterize the entire cardiac cycle. Furthermore, in order to track the 3D motion of the heart, multiple orthogonal image planes (ie, coronal, sagittal, transverse) or orthogonally motion-encoded volumes[19] need to be acquired. For this reason, tagged MR images are simultaneously acquired with an external ECG signal that allows for the triggering of the tagging prepulse and gating of the data in different cardiac phases, as can be seen in the schematic sequence in **Fig. 2**.

Once the tagged MR images have been reconstructed for each cardiac phase, different approaches can be used to estimate motion. B-spline nonrigid registration of SPAMM-tagged images has successfully been applied to track myocardial motion in PET-MR phantom studies,[5,20] and recently in a proof-of-concept clinical study[21] dividing the cardiac cycle into 9 phases.

One of the main disadvantages of tagged MR imaging is the extended time required to obtain a complete description of the motion during the cardiac cycle, so it is usually a simultaneous motion model technique. As reported,[21] the acquisition time of fully sampled tagged MR images for a patient experiment was more than 8 minutes, preventing the application of other clinically relevant sequences to assess cardiac anatomy and function. Half *k*-space acquisition,[20] compressed sensing, and parallel imaging undersampled reconstruction techniques[21] have been used to accelerate the acquisition of tagged MR images and move toward a precalibrated motion model approach. Huang and colleagues[21] demonstrated that using compressed sensing,[22] 8 times

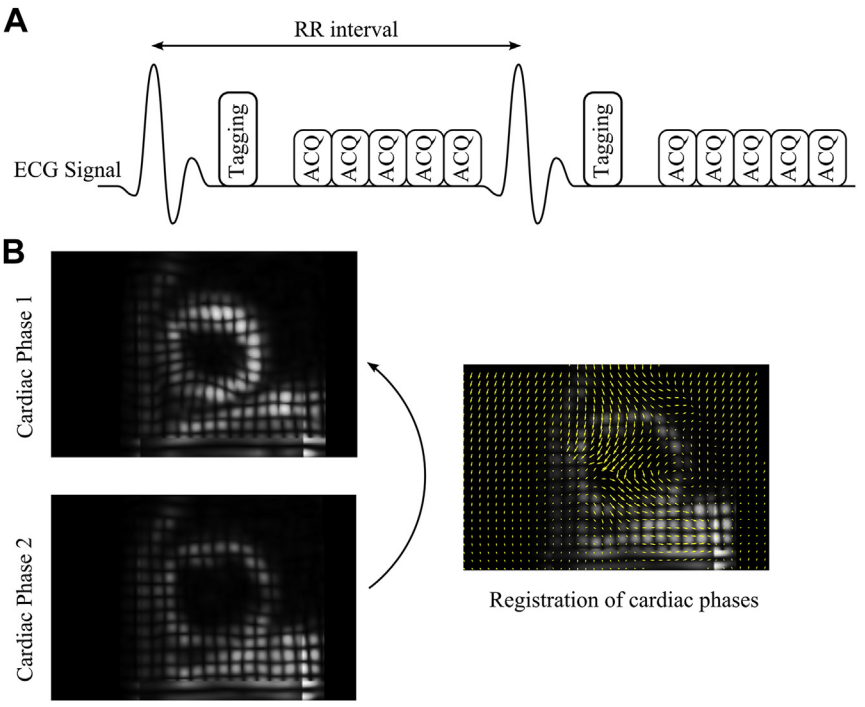

Fig. 2. (*A*) Schematic sequence of tagged MR imaging acquisition. (*B*) Two cardiac phases acquired using tagged MR images of a single ventricle patient are shown. Registration between cardiac phases provides an estimation of the motion fields.

accelerated tagged MR imaging can still provide accurate motion estimation and yield motion-corrected PET images of a similar quality to those corrected with motion estimated from fully sampled tagged MR imaging. This was demonstrated both in phantom studies and in 1 patient using myocardial defect contrast as the measurement of image quality. These preliminary results are promising; however, an increased sample size and standardized metrics of image quality for the motion-corrected PET image, such as channelized Hotelling observer (CHO),[23] are required in order to fully evaluate the performance of accelerated tagged MR imaging techniques.

Respiratory Motion

Breathing is the main source of motion in abdominal and thoracic imaging, and is a major problem in cardiac imaging. A wide variety of techniques have been proposed to estimate respiratory motion using MR images; however, this review focuses only on those that have been applied to PET-MR imaging.

As explained before, precalibrated motion model techniques aim to create a patient-specific motion model from imaging data, usually by acquiring a surrogate signal simultaneously with the imaging data, so that the model approximates the relationship between the surrogate and the motion.[6] For PET-MR imaging, precalibrated motion models are based on near real-time MR images acquired before the simultaneous PET-MR acquisition. This approach has been applied in MR-based PET simulation studies[24–29] with healthy volunteer MR data. 3D T1-weighted turbo field echo (TFE) MR images were acquired using parallel imaging (SENSE) with an acceleration factor of 8, so that each whole-thorax volume is acquired in 0.7 seconds. Motion displacements estimated from hierarchical local affine registration of these fast acquired 3D MR imaging volumes are modeled as second-order polynomial functions of a 1D surrogate signal, so that during PET-MR acquisition only information from the position of a 1D navigator echo is required for motion estimation. In the report by King and colleagues,[30] 2D images were used as surrogate for a statistical motion model, and more robust results were obtained compared with 1D surrogates.

A different precalibrated model-based approach was proposed by Würslin and colleagues[31] and tested in thoracic images of 5 patients. Here, a motion model is generated during

the first 3 minutes of simultaneous PET-MR acquisition, by acquiring multiple high-resolution 2D sagittal spoiled gradient echo MR images that are retrospectively reordered to form 4 3D volumes. During the remainder of the examination, only a 1D respiratory surrogate is acquired, which is used to retrospectively bin the acquired PET data. Motion fields are estimated by nonrigid registration of the 3D volumes to the end-expiratory volume. The investigators stated that reducing the time required for motion estimation was desirable in order to provide time for diagnostic MR sequences; however, there was no discussion about the effect of changing the time allocated for generating the motion model.

The most common simultaneous motion model approach applies nonrigid registration to images reconstructed at different respiratory bins (so-called bin-to-bin respiratory motion estimation). Similar to cardiac motion estimation, a signal related to the breathing cycle is required for retrospectively assigning the acquired data to different binning windows, so that each of the respiratory phases contains data acquired at similar respiratory positions in multiple breathing cycles. External devices can be used for this purpose, but MR imaging offers the capability of directly monitoring the hemidiaphragm position by interleaving 1D navigator echoes during MR acquisition. A navigator echo usually consists of an image of 1 thin column of tissue, obtained by applying a spatially selective excitation 2D pulse oriented in the foot-head direction, to monitor the position of the liver-lung interface. This approach has been used in 2 PET-MR patient studies. In the report by Dutta and colleagues,[32] data acquired using a golden-angle radial FLASH pulse sequence were retrospectively binned into 8 respiratory bins for thoracic imaging. In article by Petibon and colleagues,[33] data acquired using a navigated steady-state free-precession (true fast imaging with steady-state precession) MR acquisition protocol were binned into 7 bins for abdominal imaging.

Alternatively, a self-gating 1D respiratory surrogate to bin the data can be derived from the acquired data, without requiring additional interleaved echoes or external signals. A self-gating approach for respiratory motion estimation in PET-MR was proposed by Grimm and colleagues,[34,35] and evaluated in abdominal and thoracic images of 15 patients. MR data were acquired using a 3D T1-weighted golden-radial stack-of-stars spoiled gradient echo with fat suppression sequence. The stack-of-stars trajectory (**Fig. 3**) allows a respiratory signal to be derived from the center of the k-space ($k_x = k_y = 0$) for each line acquired in the central slice of the volume ($k_z = 0$). Based on this signal the MR data were retrospectively binned into 2 to 15 uniform respiratory bins. The investigators concluded that up to 10 bins are required to recover the full respiratory amplitude depending on the respiratory pattern of the patient. However, when analyzing the average binning error, using only 5 bins the 95th percentile of the error was less than 2 mm, suggesting that increasing the number of bins to more than 5 does not have a significant impact on the accuracy of the estimated motion.

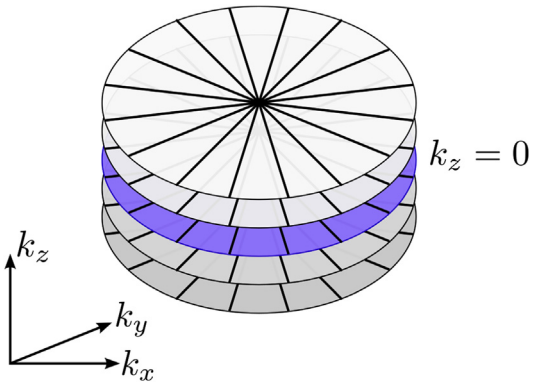

Fig. 3. The stacks-of-stars trajectory acquires radial spokes in the k_x–k_y plane and uses Cartesian sampling along the k_z direction. The angle increment between consecutively acquired spokes corresponds to the golden angle (111.246°). A respiratory signal can be estimated using the central sample of any spoke acquired in the central slice of the volume ($k_z = 0$).

Fürst and colleagues[36] compared the performance of a simultaneous motion model using 5 different 1D respiratory surrogates for retrospective binning of MR data, including respiratory bellows, an MR-based self-gated signal, and 3 PET-based navigators, finding high correlation between the different respiratory signals. This study was performed in 20 patients, who were referred for diagnosis of malignant diseases in the abdomen (11 patients), heart (1 patient), and thorax (8 patients).

A different bin-to-bin-based simultaneous motion model approach involves the acquisition of near real-time MR images that are subsequently classified in different respiratory phases. Fieseler and colleagues,[16] used an image-based navigator to select 6 respiratory phases from a set of 35 acquired 3D TFE images of a phantom capable of both cardiac and respiratory motion. A similar approach was used by Manber and colleagues[37] for 2D motion estimation, where a PET-derived respiratory signal is used to group acquired 2D real-time MR images into 10 respiratory bins. Finally, motion is estimated by nonrigid registration

between the average image of each bin and a reference image.

Tagged MR imaging has also been used to estimate respiratory motion to improve accuracy in regions with uniform contrast such as the liver. B-spline nonrigid registration of tagged MR images using 2 different similarity measures (ie, sum of squared differences and negative mutual information) has been applied to abdominal imaging of rabbits and nonhuman primates.[38] The investigators found no statistically significant difference in the detectability of lesions in motion-corrected PET images using either similarity measure. Guerin and colleagues[39] estimated motion through regularized phase-tracking of multislice tagged MR images. The proposed approach was demonstrated to be robust against noise in a numerical simulation study, but its applicability to in vivo data has not been tested. As discussed by the investigators, a severe limitation of tagged MR approaches for respiratory motion estimation is the lack of signal in the lungs.

Dual gating has been proposed to address both cardiac and respiratory motion simultaneously. Nonrigid registration of dual-gated images into a reference cardiac and respiratory phase, assuming the existence of 1D surrogates for both the cardiac-induced and respiratory-induced motion of the heart (**Fig. 4**), has been shown in simulation studies.[40,41] In the report by Tang and colleagues,[17] respiratory motion was assumed to be rigid within each cardiac phase, so rotation and translation parameters that characterize motion between respiratory phases were estimated using least squares minimization. Using these parameters, respiratory corrected MR images were reconstructed for each cardiac phase and, subsequently, nonrigid cardiac motion was estimated using optical flow.

Whereas simultaneous motion model techniques are robust for patients with irregular breathing patterns, they require continuous acquisition of motion information preventing the simultaneous acquisition of other diagnostic MR images during PET acquisition. However, precalibrated motion model techniques should allow the acquisition of different MR sequences in parallel with PET, when the required respiratory surrogate is 1D and can be obtained as part of the diagnostic MR acquisition. It is worth considering that although motion models provide near real-time motion estimates, motion correction is usually performed in a bin-to-bin framework because of computational constraints.

All previously described techniques assume that cardiac and respiratory motion is periodic, so that information about the relative position within the cardiac cycle and/or the respiratory cycle is enough to characterize the motion status of the acquired data. Nevertheless, during long examinations, images are also affected by bulk motion of the patient. The problem of detecting and

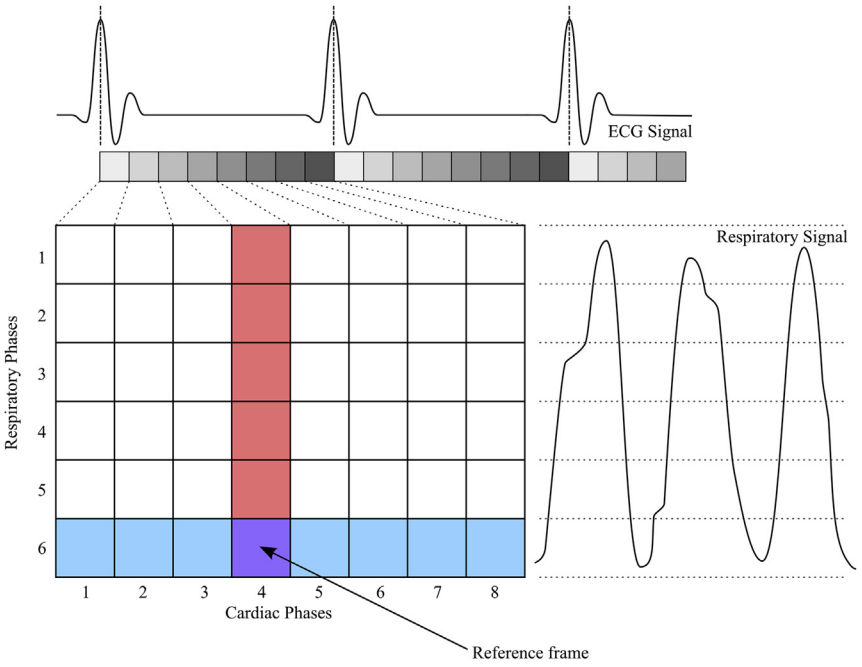

Fig. 4. Simultaneous cardiac and respiratory motion estimation from dual-gated MR data. Each motion-free frame is registered to a reference frame, usually end expiration and end-diastole.

estimating bulk motion in PET-MR has been addressed in a PET simulation study based on abdominal MR data from 3 healthy volunteers.[42] In vivo studies are required to assess the impact of bulk motion correction.

PET MOTION CORRECTION

MR-based estimated motion fields can be applied in 2 different ways to compensate for nonrigid motion in PET images. In the first, each motion-free frame is reconstructed independently, and inverse motion transformations are used to warp PET images from different motion states to a common reference position. This approach is variously known as postreconstruction registration (PRR), reconstruct-register-average, or reconstruct-transform-average.[43] The second approach incorporates the motion information directly into the system matrix of the iterative PET reconstruction algorithm, and is known as motion-compensated image reconstruction (MCIR).[44]

Postreconstruction Registration

In order to reconstruct each frame separately, PRR approaches apply binning to the acquired PET data with the same gating signal and bins used for motion estimation. Usually, each frame is reconstructed using the standard ordered-subsets expectation-maximization (OSEM) algorithm.[45] Attenuation correction maps for each bin are computed from a static reference map by applying the corresponding motion transformation. Once all frames have been reconstructed, they are transformed back to the reference frame, usually end expiration and end-diastole, and ultimately averaged (**Fig. 5**).

This approach has been applied in simulation studies with a numerical phantom[40] and PET simulations based on real MR data.[24,25,46,47] Studies reported improvements in accuracy of uptake values in lesions and regions of interest (ROIs),[24,25] increased contrast (72.17%) and SNR (63.8%) for manually defined ROIs,[47] and increased normalized cross-correlation[46] compared with uncorrected images. When applied to real PET-MR data from phantoms,[16,48] a significant reduction in image artifacts has been reported. Preliminary studies on patients[31,34] reported increased SNR (28.1%) and reduction in apparent lesion volume (11.8%–26.5%) compared with uncorrected images, but reduced contrast (−11.3%) compared with gated images. As discussed by Würslin and colleagues,[31] the loss of contrast is probably related to remnant intrabin motion that reduces the quality of the images reconstructed at each respiratory phase, and ultimately

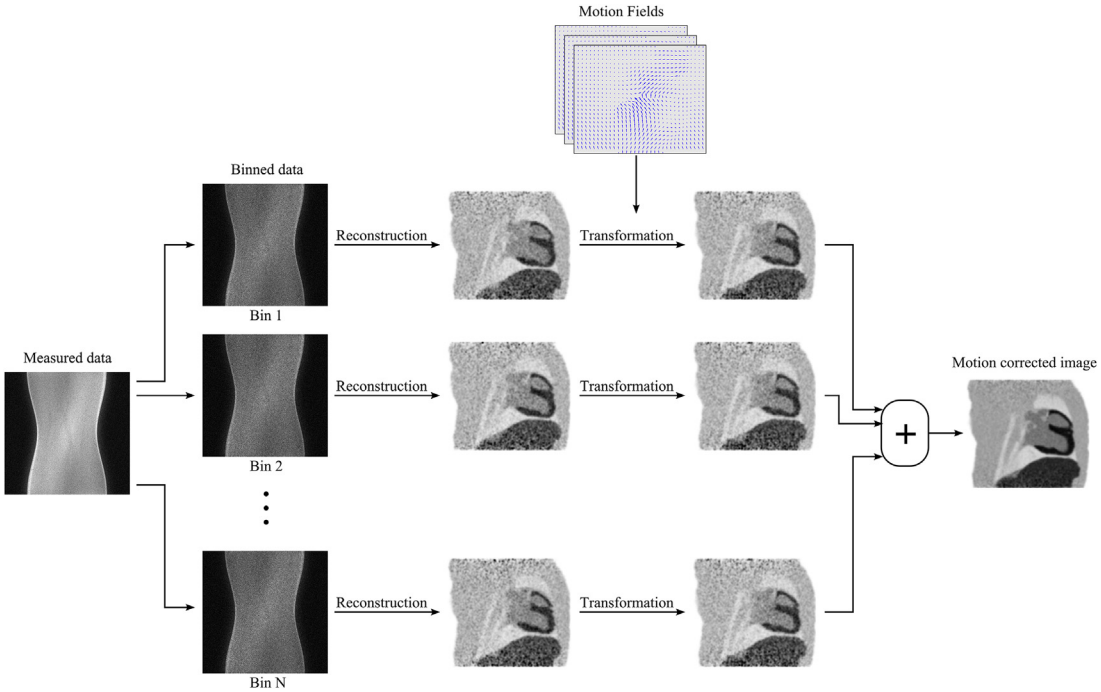

Fig. 5. Postreconstruction registration approach. The measured data are binned into *N* motion-free frames, which are reconstructed separately. Reconstructed images are then transformed to a reference frame using motion estimates, and finally averaged to obtain the final motion-corrected image.

induces blurring in the combined motion-corrected PET image (**Fig. 6**).

Instead of using the average of the back-transformed reconstructed frames, Grimm and colleagues[35] proposed the use of a weighted sum that takes into account the differences in image quality between frames. The weighting factor is inversely proportional to the intrabin amplitude range, so that quiescent respiratory gates such as end expiration have more influence in the final image than end-inspiratory data. However, results reported for lesions in 15 clinical patients still show reduced contrast ($-10.3 \pm 12.0\%$) compared with gated images (**Fig. 7**).

Motion-Corrected Image Reconstruction

Theoretically, once motion is available throughout the PET acquisition, PET data could be corrected by incorporating the transformation between the current and a reference position into any iterative reconstruction algorithm. However, in order to avoid increasing reconstruction time significantly, PET data are binned (**Fig. 8**). The widely used OSEM algorithm can be modified to include motion information in the system matrix, modifying both the emission and attenuation maps, as shown in Equation 1.[41] Accidental coincidences (ie, random and scatters) are usually assumed to vary slowly compared with the emission map, so the effect of motion on them is neglected.

$$\rho^{(iter+1)} = \frac{\rho^{(iter)}}{\sum_k (M^k)^T P^T N A^k 1_I} \times \sum_k (M^k)^T P^T \frac{s^k_{tot}}{PM^k \rho^{(iter)} + (A^k N)^{-1}(\overline{sc} + \overline{r})} \quad (1)$$

where ρ is a column vector that contains the PET voxel values in the reference phase, M^k is a motion operator that transforms an image at the reference phase to a phase k, P is a matrix that models the system forward-projection, N is a diagonal matrix with entries down the diagonal equal to the reciprocal of the normalization-correction factors, A^k is a diagonal matrix with entries down the diagonal equal to the reciprocal of the attenuation correction factors for phase k, s^k_{tot} is a column vector that contains counts detected in phase k, and $\overline{sc}$, $\overline{r}$ represent estimations of scattered and random coincidences, respectively.

This approach has been applied in simulation studies with numerical phantoms,[28,49] PET simulation based on MR data of healthy volunteers,[41] PET-MR data acquired from phantoms,[20,39] animal studies,[5,38] and small studies on oncological and cardiac patients.[21,33,36,37] Phantom and animal studies reported that motion correction can improve contrast by 21% to 280% and lesion detectability by 19% to 235% compared with uncorrected images, and improves lesion detectability (65%–276%) compared with gated images. The wide range of improvement is probably related to the wide range of motion amplitudes studied. In

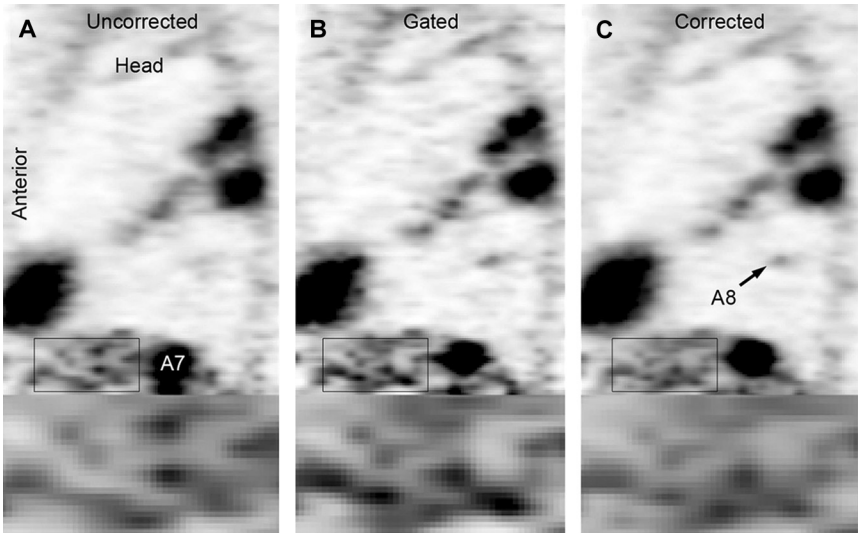

Fig. 6. Comparison of uncorrected (*A*), gated (*B*), and corrected (*C*) sagittal PET image slice of a lung with multiple lesions. Lesion (A8) is enhanced in gated and corrected images. Box indicates the zoomed region at bottom of the Figure. (This research was originally published in *JNM*. Würslin C, Schmidt H, Martirosian P, et al. Respiratory motion correction in oncologic PET using T1-weighted MR imaging on a simultaneous whole-body PET/MR system. J Nucl Med 2013;54(3):464–7. © by the Society of Nuclear Medicine and Molecular Imaging, Inc.)

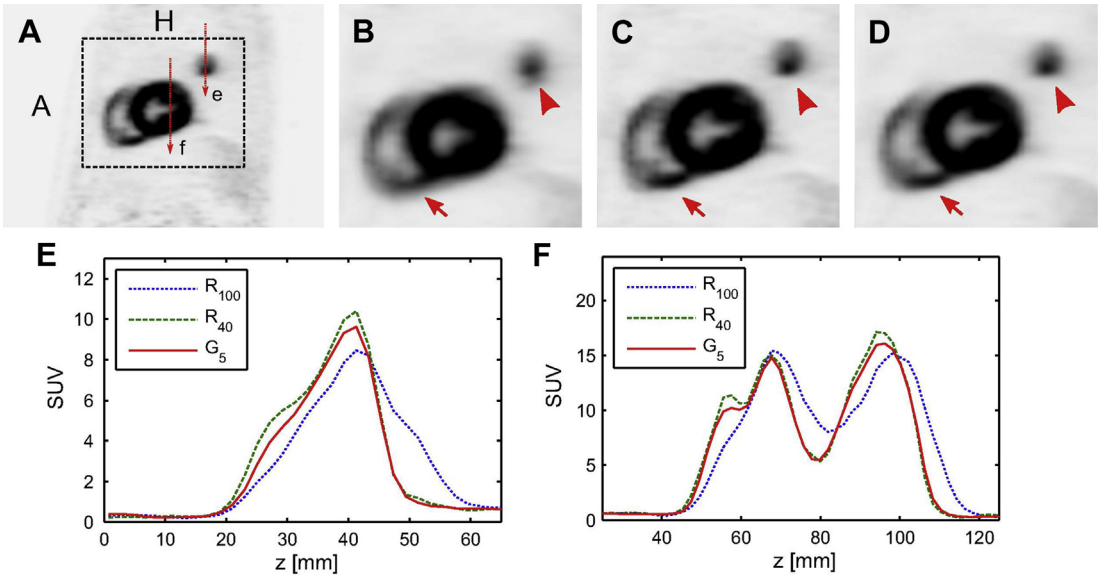

Fig. 7. (*A*) Sagittal slice through heart, (*B*) uncorrected image (R100), (*C*) gated image (R40), (*D*) motion-corrected image (G5). Motion correction reduces blurring compared with uncorrected reconstruction, but the contrast is not fully recovered as can be seen in the profiles through (*E*) the lesion (*arrowhead*) and (*F*) the myocardium (*arrow*). (*From* Grimm R, Fürst S, Souvatzoglou M, et al. Self-gated MRI motion modeling for respiratory motion compensation in integrated PET/MRI. Med Image Anal 2014;19:117; with permission.)

regions where motion is large, motion correction could have more impact than in regions with small or no motion. For patients, the results reported show an increase in the lesion uptake value of 11% to 23%, a reduction in the apparent lesion volume of 12% to 29%, and an increase in the SNR of 21% to 44% in comparison with uncorrected images. An example of the impact of motion correction in liver lesion detection can be seen in **Fig. 9**.[20] Improvements in contrast without SNR loss are apparent in the motion-corrected image. Besides motion-compensated OSEM, iterative motion-compensated maximum a posteriori (MAP) image reconstruction has also been proposed.[32]

Tang and colleagues[17] used a combination of PRR and MCIR approaches. For a dual-gated simulated PET-MR dataset, each cardiac phase was reconstructed using respiratory motion-compensated OSEM, and then cardiac phases were transformed and averaged to obtain the final image. The investigators found improved lesion detectability for motion-corrected images compared with uncorrected data (12.9%), and for each respiratory corrected cardiac gate compared with dual-gated images (21.4%).

Comparison Between Motion-Compensated Image Reconstruction and Postreconstruction Registration

To summarize, all studies reviewed report that MR-based cardiac and respiratory motion-correction techniques reduce image blurring and improve contrast recovery compared with non–motion-corrected reconstruction, and improve SNR, and lesion detectability compared with gated reconstruction.

Of the available literature, approximately half used MCIR. Only simulation studies have compared the performance of both approaches. In a preliminary study by Dikaios and Fryer[50] based on pseudo-PET images generated from real abdominal and thoracic MR data, less bias in organ uptake values was obtained using MCIR. Using PET simulations based on MR data of 2 volunteers in a more recent study,[51] they concluded that PRR produces greater resolution loss than MCIR, but they have comparable performance in terms of global similarity indices (root mean squared error, correlation coefficient, and normalized mutual information) with respect to a motion-free gold standard.

Polycarpou and colleagues[26,27] and Tsoumpas and colleagues[29] also performed a comparison between the 2 approaches using OSEM reconstruction in an MR-based PET simulation study. They found that MCIR achieves better contrast and smaller bias in low-activity regions compared with PRR, but has lower SNR. For a small number of iterations (ie, 1–2), MCIR has better performance in terms of mean squared error (MSE) than PRR. However, as the number of iterations increases, PRR has significantly less MSE than

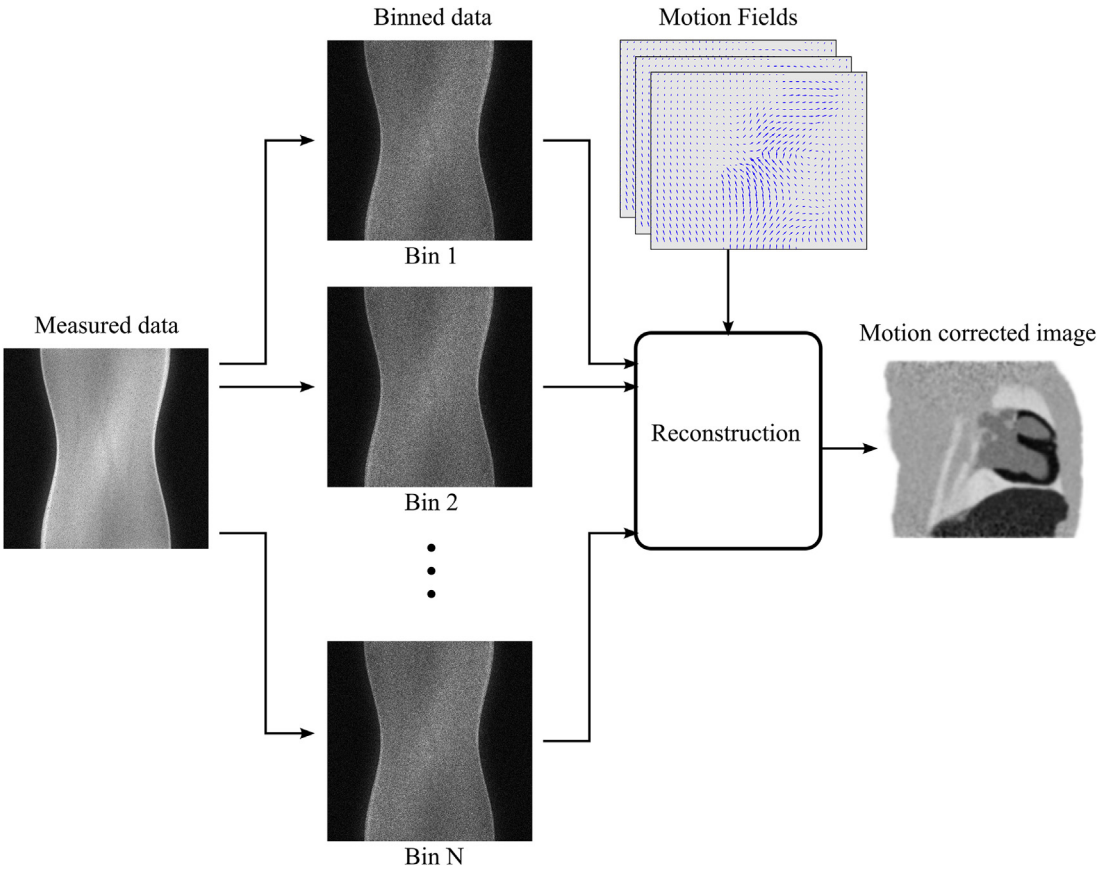

Fig. 8. Motion-compensated image reconstruction approach. The iterative reconstruction algorithm is modified in order to include motion information, modifying both the emission and attenuation maps. Usually, data are binned into motion-free frames to reduce computational burden of the reconstruction.

MCIR. This suggests that in cases where SNR is high, MCIR may provide better performance. Alternatively, regularization methods can be incorporated in PET reconstruction to control noise levels. As shown in an MR-based PET simulation study,[52] when using the ordered-subsets MAP 1-step-late algorithm with median-root-prior, MCIR with optimized regularization parameters achieves less bias and MSE, and similar contrast and SNR compared with regularized PRR.

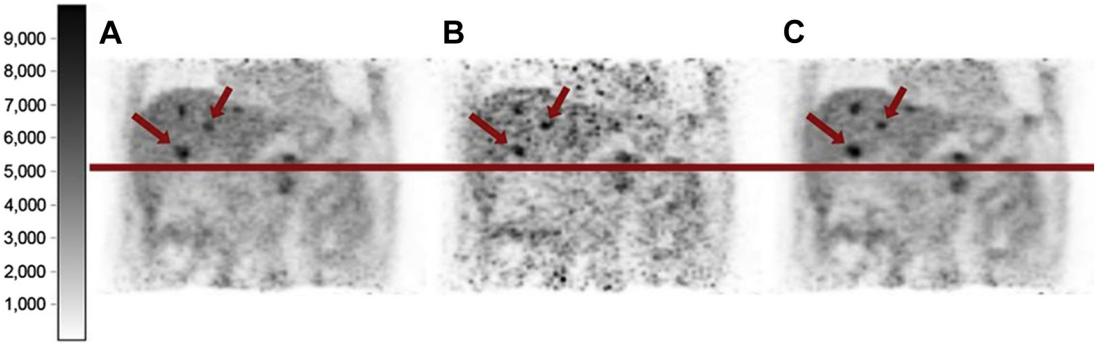

Fig. 9. Coronal slices of uncorrected (*A*), gated (*B*), and motion-corrected (*C*) images of liver with multiple lesions (*arrows*). Motion blurring of lesions was significantly reduced by gating and motion correction; however, increased noise in the gated image reduces lesion detectability. (This research was originally published in *JNM*. Fürst S, Grimm R, Hong I, et al. Motion correction strategies for integrated PET/MR. J Nucl Med 2015;56(2):261–9. © by the Society of Nuclear Medicine and Molecular Imaging, Inc.)

RELATIVE IMPACT OF MOTION CORRECTION

Preliminary studies to assess the relative impact of motion correction compared with other factors that affect the quality of PET images have been performed. Buerger and colleagues[24] compared the impact of motion and errors in the attenuation map in a PET simulation study using real MR data from 5 healthy volunteers, finding that both have a similar effect on standardized uptake values. Petibon and colleagues[33] studied the impact of including a spatially dependent model of the point spread function (PSF) into the reconstruction, testing 4 reconstruction algorithms in abdominal images of 3 patients: standard OSEM, OSEM with PSF modeling, motion-corrected OSEM, and OSEM with both PSF modeling and motion correction. The investigators concluded that the enhancement offered by PSF modeling in terms of FWHM and SNR is more significant when correcting for motion at the same time. Finally, Polycarpou and colleagues[28,49] simulated different scanner resolutions (3 and 6 mm), finding that the benefit of having higher scanner resolution is small unless motion-correction techniques are applied.

AREAS OF FUTURE RESEARCH

MR-based motion correction for PET-MR imaging is an emerging field of research, and several questions about performance and the impact of proposed approaches still remain unanswered. Most of the revised techniques have been validated in simulations, ad hoc phantoms, or small patient cohorts. Studies with standardized thoracic and abdominal phantoms capable of cardiac and/or respiratory motion are required to validate motion-estimation techniques and the accuracy of motion-corrected images.

Different clinical applications of PET have different image quality requirements. For example, lesion detectability and accurate uptake values are relevant in oncological applications, whereas improved spatial resolution is essential for some cardiovascular applications such as coronary artery imaging. For this reason, application-specific studies with larger sample sizes are required to evaluate the impact of motion correction.

Another issue that needs to be addressed is the optimal number of respiratory and cardiac phases. Reported techniques have used 4 to 8 respiratory bins and 8 to 25 cardiac gates. Grimm and colleagues[34,35] studied the average binning error for different numbers of respiratory bins; however, the impact on the motion-corrected PET image was not addressed.

In most studies, motion fields are estimated only from MR data. Motion fields estimated from both PET and MR data have been used in a simulation study,[40] showing local improvements in motion-estimation accuracy near lesions and other regions with significant tracer uptake. The impact of this technique in real PET-MR data remains to be studied.

Finally, state-of-the-art literature in PET-MR motion correction only uses MR data for motion-estimation purposes. In most cases, motion fields estimated from MR have been used to correct PET data, but no correction is performed in the simultaneously acquired MR data. Kolbitsch and colleagues[42] reported a scheme for bulk motion compensation of both PET and MR images; however, this approach has not been applied to cardiac or respiratory motion. A different approach has been proposed,[53] whereby motion is jointly estimated during MR image reconstruction, and subsequently applied to correct simulated PET data. Furthermore, design of MR protocols and techniques that make the acquisition of information useful for both motion estimation and diagnosis is still an open area.

SUMMARY

In this article, techniques that estimate cardiac and respiratory motion from MR data to perform motion correction of PET images in the context of cardiac, thoracic, and abdominal PET-MR imaging have been reviewed.

Different techniques have been proposed to obtain estimates of cardiac and respiratory motion. For abdominal and thoracic imaging, precalibrated motion models and simultaneously acquired motion models are the most common approaches for respiratory motion estimation. For cardiac imaging, some approaches only address cardiac motion through nonrigid registration of tagged or cine-MR images gated with an external ECG device. In order to include respiratory motion of the heart, nonrigid registration of dual-gated MR images has been used.

Once an estimate of the motion is available, 2 approaches to correct PET data have been proposed. In PRR, each motion-free frame is reconstructed independently, and images are then combined using motion estimates. However, in MCIR, the motion information is directly incorporated into the system matrix directly reconstructing a motion-corrected image. Using either of them significantly increases lesion detectability and contrast without SNR loss. In addition, improved accuracy of uptake values has been

reported for simulation, phantom, and preclinical as well as preliminary patient studies.

REFERENCES

1. Rahmim A, Rousset O, Zaidi H. Strategies for motion tracking and correction in PET. PET Clin 2007;2(2):251–66.
2. Papathanassiou D, Becker S, Amir R, et al. Respiratory motion artefact in the liver dome on FDG PET/CT: comparison of attenuation correction with CT and a caesium external source. Eur J Nucl Med Mol Imaging 2005;32(12):1422–8.
3. Liu C, Pierce LA, Alessio AM, et al. The impact of respiratory motion on tumor quantification and delineation in static PET/CT imaging. Phys Med Biol 2009;54(24):7345–62.
4. Nehmeh SA, Erdi YE, Ling CC, et al. Effect of respiratory gating on quantifying PET images of lung cancer. J Nucl Med 2002;43(7):876–81.
5. Ouyang J, Li Q, El Fakhri G. Magnetic resonance-based motion correction for positron emission tomography imaging. Semin Nucl Med 2013;43(1):60–7.
6. McClelland JR, Hawkes DJ, Schaeffter T, et al. Respiratory motion models: a review. Med Image Anal 2013;17(1):19–42.
7. Schleyer PJ, O'Doherty MJ, Barrington SF, et al. Retrospective data-driven respiratory gating for PET/CT. Phys Med Biol 2009;54(7):1935–50.
8. Klein GJ, Reutter BW, Huesman RH. Four-dimensional affine registration models for respiratory-gated PET. IEEE Trans Nucl Sci 2001;48(3):756–60.
9. Ambwani S, Karl WC, Tawakol A, et al. Joint cardiac and respiratory motion correction and super-resolution reconstruction in coronary PET/CT. Presented at the 2011 IEEE International Symposium on Biomedical Imaging: From Nano to Macro. Chicago, IL, March 30 – April 2, 2011. p. 1702–5.
10. Nehmeh SA, Erdi YE. Respiratory motion in positron emission tomography/computed tomography: a review. Semin Nucl Med 2008;38(3):167–76.
11. McQuaid SJ, Lambrou T, Cunningham VJ, et al. The application of a statistical shape model to diaphragm tracking in respiratory-gated cardiac pet images. Proc IEEE 2009;97(12):2039–52.
12. McQuaid SJ, Lambrou T, Hutton BF. A novel method for incorporating respiratory-matched attenuation correction in the motion correction of cardiac PET-CT studies. Phys Med Biol 2011;56(10):2903–15.
13. Fayad HJ, Pan T, Roux C, et al. A generic respiratory motion model for motion correction in PET/CT. Presented at the IEEE Nuclear Science Symposuim & Medical Imaging Conference. Knoxville, TN, October 30 – November 6, 2010. p. 2455–8.
14. Quick HH. Integrated PET/MR. J Magn Reson Imaging 2014;39(2013):243–58.
15. Wang H, Amini AA. Cardiac motion and deformation recovery from MRI: a review. IEEE Trans Med Imaging 2012;31(2):487–503.
16. Fieseler M, Kugel H, Gigengack F, et al. A dynamic thorax phantom for the assessment of cardiac and respiratory motion correction in PET/MRI: a preliminary evaluation. Nucl Instrum Methods Phys Res A 2012;702:59–63.
17. Tang J, Hall N, Rahmim A. MRI assisted motion correction in dual-gated 5D myocardial perfusion PET imaging. Presented at the 2012 IEEE Nuclear Science Symposium and Medical Imaging Conference Record (NSS/MIC). Anaheim, CA, October 27 – November 3, 2012. p. 4054–7.
18. Axel L, Dougherty L. MR imaging of motion with spatial modulation of magnetization. Radiology 1989;171(3):841–5.
19. Rutz AK, Ryf S, Plein S, et al. Accelerated whole-heart 3D CSPAMM for myocardial motion quantification. Magn Reson Med 2008;59(4):755–63.
20. Petibon Y, Ouyang J, Zhu X, et al. Cardiac motion compensation and resolution modeling in simultaneous PET-MR: a cardiac lesion detection study. Phys Med Biol 2013;58(7):2085–102.
21. Huang C, Petibon Y, Ouyang J, et al. Accelerated acquisition of tagged MRI for cardiac motion correction in simultaneous PET-MR: phantom and patient studies. Med Phys 2015;42(2):1087–97.
22. Lustig M, Donoho D, Pauly JM. Sparse MRI: the application of compressed sensing for rapid MR imaging. Magn Reson Med 2007;58(6):1182–95.
23. Barrett HH, Yao J, Rolland JP, et al. Model observers for assessment of image quality. Proc Natl Acad Sci U S A 1993;90(21):9758–65.
24. Buerger C, Tsoumpas C, Aitken A, et al. Investigation of MR-based attenuation correction and motion compensation for hybrid PET/MR. IEEE Trans Nucl Sci 2012;59(5):1967–76.
25. King AP, Tsoumpas C, Buerger C, et al. Real-time respiratory motion correction for simultaneous PET-MR using an MR-derived motion model. Presented at the 2011 IEEE Nuclear Science Symposium and Medical Imaging Conference. Valencia, October 23–29, 2011. p. 3589–94.
26. Polycarpou I, Tsoumpas C, Marsden PK. Analysis and comparison of two methods for motion correction in PET imaging. Med Phys 2012;39(10):6474–83.
27. Polycarpou I, Tsoumpas C, Marsden PK. Statistical evaluation of PET motion correction methods using MR derived motion fields. In IEEE Nuclear Science Symposium Conference. Valencia, October 23–29, 2011. p. 3579–85.
28. Polycarpou I, Tsoumpas C, King AP, et al. Impact of respiratory motion correction and spatial resolution on lesion detection in PET: a simulation study based on real MR dynamic data. Phys Med Biol 2014;59(3):697–713.

29. Tsoumpas C, Agarwal S, Marsden PK, et al. Evaluation of two PET motion correction techniques for simultaneous real-time PET-MR acquisitions using an MR-derived motion model. Presented at the IEEE Nuclear Science Symposium Conference. Anaheim, CA, October 27 – November 3, 2012. p. 2519–22.
30. King AP, Buerger C, Tsoumpas C, et al. Thoracic respiratory motion estimation from MRI using a statistical model and a 2-D image navigator. Med Image Anal 2012;16(1):252–64.
31. Würslin C, Schmidt H, Martirosian P, et al. Respiratory motion correction in oncologic PET using T1-weighted MR imaging on a simultaneous whole-body PET/MR system. J Nucl Med 2013;54(3):464–71.
32. Dutta J, El Fakhri G, Huang C, et al. Respiratory motion compensation in simultaneous PET/MR using a maximum a posteriori approach. Presented at the 2013 IEEE 10th International Symposium on Biomedical Imaging. San Francisco, CA, April 7–11, 2013. p. 800–3.
33. Petibon Y, Huang C, Ouyang J, et al. Relative role of motion and PSF compensation in whole-body oncologic PET-MR imaging. Med Phys 2014;41(4):042503.
34. Grimm R, Fürst S, Dregely I, et al. Self-gated radial MRI for respiratory motion compensation on hybrid PET/MR systems. In: Mori K, Sakuma I, Sato Y, et al, editors. Medical image computing and computer-assisted intervention – MICCAI 2013 SE - 3, vol. 8151. Berlin; Heidelberg (Germany): Springer; 2013. p. 17–24.
35. Grimm R, Fürst S, Souvatzoglou M, et al. Self-gated MRI motion modeling for respiratory motion compensation in integrated PET/MRI. Med Image Anal 2014;19(1):110–20.
36. Fürst S, Grimm R, Hong I, et al. Motion correction strategies for integrated PET/MR. J Nucl Med 2015;56:261–9.
37. Manber R, Thielemans K, Hutton BF, et al. Initial evaluation of a practical PET respiratory motion correction method in clinical simultaneous PET/MRI. EJNMMI Phys 2014;1(Suppl 1):A40.
38. Chun SY, Reese TG, Ouyang J, et al. MRI-based nonrigid motion correction in simultaneous PET/MRI. J Nucl Med 2012;53(8):1284–91.
39. Guerin B, Cho S, Chun SY, et al. Nonrigid PET motion compensation in the lower abdomen using simultaneous tagged-MRI and PET imaging. Med Phys 2011;38(6):3025–38.
40. Fieseler M, Gigengack F, Jiang X, et al. Motion correction of whole-body PET data with a joint PET-MRI registration functional. Biomed Eng Online 2014;13(Suppl 1):S2.
41. Petibon Y, El Fakhri G, Nezafat R, et al. Towards coronary plaque imaging using simultaneous PET-MR: a simulation study. Phys Med Biol 2014;59(5):1203–22.
42. Kolbitsch C, Prieto C, Tsoumpas C, et al. A 3D MR-acquisition scheme for nonrigid bulk motion correction in simultaneous PET-MR. Med Phys 2014;41(8):082304.
43. Picard Y, Thompson CJ. Motion correction of PET images using multiple acquisition frames. IEEE Trans Med Imaging 1997;16(2):137–44.
44. Qiao F, Pan T, Clark JW, et al. A motion-incorporated reconstruction method for gated PET studies. Phys Med Biol 2006;51(15):3769–83.
45. Hudson HM, Larkin RS. Accelerated image reconstruction using ordered subsets of projection data. IEEE Trans Med Imaging 1994;13(4):601–9.
46. Miao S, Liao R, Moran G, et al. Dynamic MR-based respiratory motion compensation for hybrid PET/MR system. Presented at the 9th IEEE Conference on Industrial Electronics and Applications. Hangzhou, June 9–11, 2014. p. 1915–20.
47. Fayad HJ, Odille F, Felblinger J, et al. A generic PET/MRI respiratory motion correction using a generalized reconstruction by inversion of coupled systems (GRICS) approach. Presented at the 2012 IEEE Nuclear Science Symposium and Medical Imaging Conference Record (NSS/MIC). Anaheim, CA, October 27 – November 3, 2012. p. 2813–6.
48. Tsoumpas C, Mackewn JE, Halsted P, et al. Simultaneous PET-MR acquisition and MR-derived motion fields for correction of non-rigid motion in PET. Ann Nucl Med 2010;24(10):745–50.
49. Polycarpou I, Tsoumpas C, King AP, et al. Quantitative evaluation of PET respiratory motion correction using real- time PET/MR simulated data. EJNMMI Phys 2014;1(Suppl 1):A62.
50. Dikaios N, Fryer TD. Respiratory motion correction of PET using motion parameters from MR. Presented at the 2009 IEEE Nuclear Science Symposium Conference Record (NSS/MIC). Orlando, FL, October 24 – November 1, 2009. p. 2806–8.
51. Dikaios N, Izquierdo-Garcia D, Graves MJ, et al. MRI-based motion correction of thoracic PET: initial comparison of acquisition protocols and correction strategies suitable for simultaneous PET/MRI systems. Eur Radiol 2012;22(2):439–46.
52. Tsoumpas C, Polycarpou I, Thielemans K, et al. The effect of regularization in motion compensated PET image reconstruction: a realistic numerical 4D simulation study. Phys Med Biol 2013;58(6):1759–73.
53. Fayad HJ, Odille F, Schmidt H, et al. The use of a generalized reconstruction by inversion of coupled systems (GRICS) approach for generic respiratory motion correction in PET/MR imaging. Phys Med Biol 2015;60(6):2529–46.